Chem Biol Drug Des 2011; **78:** 85–93

Research Article

doi: 10.1111/j.1747-0285.2011.01099.x

Interaction of Acylated and Substituted Antimicrobial Peptide Analogs with Phospholipid–Polydiacetylene Vesicles. Correlation with their Biological Properties

Alvaro Siano[1,†], María V. Húmpola[1,†], María C. Rey[1,2], Arturo Simonetta[2], and Georgina G. Tonarelli[1,*]

[1]*Departamento de Química Orgánica, Facultad de Bioquímica y Cs. Biológicas, Universidad Nacional del Litoral (U.N.L). Ciudad Universitaria, Santa Fe, Argentina*

[2]*Cátedras de Microbiología y Biotecnología, Departamento de Ingeniería en Alimentos, Facultad de Ingeniería Química, U.N.L. Santiago del Estero 2829, Santa Fe, Argentina*

**Corresponding author: Georgina G. Tonarelli, tonareli@fbcb.unl.edu.ar*

[†]*Both authors contributed equally to this work.*

A series of peptide analogs based on region 6–22 of Plantaricin 149 sequence were synthesized. The interaction between these analogs and phospholipid–polydiacetylene vesicles was investigated to evaluate the ability of the bioassay to detect differences in the interaction of the peptides with dipalmitoylphosphatidylglycerol and dipalmitoylphosphatidylcholine vesicles, associated with amino acid substitution and N-terminal conjugation of the sequences with short fatty acids (8 and 12 carbon atoms). Fatty acid conjugation of peptides with low antimicrobial activity resulted in lipopeptides with improved activity against strains of *Staphylococcus aureus* and *Listeria monocytogenes*. The length of the fatty acid determined the bacterial specificity, and the conjugation with n-octanoic acid yielded the most active analog (C8-CT) against *Staphylococcus aureus* strain (MIC: 1.0 μM) while the conjugation with n-dodecanoic acid (C12-CT) was optimal for *Listeria monocytogenes* strain (MIC: 2.0 μM). In contrast, the substitution of Phe by Trp had an unfavorable effect on the antimicrobial activity. Hemolysis tests and membrane interaction studies with dipalmitoylphosphatidylcholine–polydiacetylene vesicles showed that lipopeptides interact to a greater extent with both biological and biomimetic membranes. Also, a good correlation was found between antimicrobial activity against *Staphylococcus aureus* strain and % colorimetric response values with dipalmitoylphosphatidylglycerol–polydiacetylene vesicles.

Key words: antimicrobial activity, bioassays, hemolysis, liposomes, PDA, peptides, phospholipids

Received 22 October 2010, revised 7 January 2011 and accepted for publication 27 January 2011

Abbreviations: ACN, acetonitrile; AMP, antimicrobial peptides; DMF, dimethylformamide; DPPC, dipalmitoylphosphatidylcholine; DPPG, dipalmitoylphosphatidylglycerol; EDT, ethanedithiol; Fmoc, fluoren-9-ylmethoxycarbonyl; MIC, minimal inhibitory concentration; PDA, polydiacetylene; TFA, trifluoroacetic acid; TFE, trifluoroethanol; TIS, triisobutylsilane.

The emergence of bacterial strains resistant to conventional antibiotics is one of the major causes of inefficient therapy and high mortality rates. For this reason, intensive efforts are being made to develop novel drugs targeting bacterial cell membranes. Short antimicrobial peptides (10–30 residues) are prevalent in nature as part of the intrinsic defense mechanism of most organisms and have been proposed as models for the design of novel antimicrobial agents (1). This has led to the proliferation of new technologies for drug discovery, which requires the parallel development of new techniques to allow the rapid screening of large number of chemical and biological compounds.

Given the structural complexity of the membrane of actual cells and the difficulties encountered in working with complex cellular systems, the study of peptide–membrane interactions using model systems such as liposomes or micelles becomes primordial. These artificial models further allow examining the contribution of specific parameters to membrane–peptide interactions and peptide activities. In this way, molecular assemblies containing synthetic conjugated polymers and lipids offer a unique platform for their application as biosensors (2,3).

Conjugated substituted diacetylenes with various side chains readily undergo photopolymerization via 1,4-addition reaction to form a ene-yne alternated polymer chain under UV irradiation in a wide range of organized structures, such as single crystal, Langmuir–Blodgett (LB) films, self-assembled monolayers, liposomes or vesicles (4–10).

Polydiacetylene (PDA) optical absorption occurs via a $\pi \rightarrow \pi^*$ electronic transition within the linear π-conjugated polymer backbone.

The polymer backbone has two spectroscopically distinct phases, designated as the blue and the red forms, which result from their excitation absorption peaks at 650 and 540 nm, respectively. Under a variety of environmental perturbations, such as temperature, pH, surface pressure or mechanical stress, the PDA backbone can undergo a drastic color transition from the blue to the red form (11–13). Research work carried out by Jelinek's group has shown that mixed vesicles containing both natural lipids and PDA could serve as a membrane-mimicking environment for the detection of interfacial processes (3,14). A detailed biophysical study of these biomimetic membrane assemblies was also reported (15).

Many lactic acid bacteria secrete ribosomally synthesized antimicrobial peptides, known as bacteriocins. These peptides are usually cationic, membrane permeabilizing, and contain between 25 and 60 amino acid residues (16). Plantaricin 149 is a bacteriocin produced by *Lactobacillus plantarum* NRIC 149 isolated from pineapple (17). We have previously demonstrated the bactericidal activity of a synthetic carboxamide analog of Plantaricin 149 (Pln149a) against strains of gram (+) food-borne pathogenic bacteria (18). Also, the ability of Pln149a to inhibit *S. cerevisiae* growth was reported (19).

In this work, we investigated the interaction of truncated and modified analogs of Pln149a with PDA–phospholipid vesicles to evaluate the ability of the bioassay to detect differences in the interaction of the peptides with the vesicles. These results were compared with those obtained in the biological assays. The antimicrobial activity of the peptides against two strains of gram (+) bacteria, *Staphylococcus aureus* and *Listeria monocytogenes*, and the cytotoxic activity against human red blood cells were also investigated.

The two gram (+) bacteria under study contain a predominance of phosphatidylglycerol in their membranes. *Listeria* membranes contain 30% lipids, 80% of which correspond to phospholipids (20), while *S. aureus* has around 25% lipids, more than 95% being phospholipids (21). The different compositions of these biological membranes indicate that different peptides can interact differently to produce their permeabilization.

Materials and Methods

Peptide synthesis

Plantaricin 149 analog (Pln149a), CT (region 6–22 of Pln149a), CT[W17] corresponding to a CT substituted analog where Phe17 was replaced by Trp17, and N-terminal fatty acid-acylated analogs of CT (with n-octanoic and n-dodecanoic acid) (see Table 1) were synthesized by Fmoc solid-phase synthesis (SPPS) as C-terminal amides.

Couplings were performed by O-(Benzotriazol-1-yl)-*N,N,N′,N′*-tetramethyluronium tetrafluoroborate (TBTU) and diisopropylethylamine (DIEA). Fmoc-deblockings were performed with 20% piperidine in DMF (v/v).

Final cleavage from the resin was achieved by a mixture of TFA/H_2O/EDT/TIS (94.5: 2.5: 2.5: 0.5) (v/v). After 3 h, the resin was filtered off, and the crude peptide was precipitated in dry cold diethyl ether, centrifuged, and washed several times with cold diethyl ether until scavengers were removed. The product was then dissolved in water and lyophilized twice. Peptides were purified by HPLC (Gilson, France) using a semi-preparative reverse-phase C18 column (Jupiter-Proteo Phenomenex, 10 μm, 90 Å, 250 × 10 mm).

The purified peptides were analyzed by analytical RP-HPLC using a Jupiter (Phenomenex, Torrence, CA, USA) C4 column (5 μm, 300 Å, 250 × 4.60 mm,). The peptides were eluted with a linear gradient of 5–80% of acetonitrile with 0.1% TFA at flow rate of 0.8 mL per min for 33 min. The absorbance was measured at 220 nm. The experimental molecular weights were determined using an Ultraflex II Bruker Daltonics MALDI-TOF/TOF mass spectrometer.

Minimal inhibitory concentration (MIC) determination

Minimal inhibitory concentration (MIC) determinations were performed by the modified microtiter dilution assay, according to the procedures proposed by R.E.W. Hancock Laboratory for testing antimicrobial peptides (http://cmdr.ubc.ca/bobh/methods/MODIFIED-MIC.html). *Listeria monocytogenes* DBFIQ LM 3 and *S. aureus* DBFIQ S 21 strains, both belonging to the culture collection of Cátedras de Microbiología y Biotecnología – FIQ-UNL (DBFIQ), were activated by culture for 24 h at 37 °C on Mueller–Hinton broth (MHB) (Biokar Diagnostics). In these cultures, cellular concentrations were of 5×10^7 CFU/mL. These inocula were used to perform the assay in coated glass tubes using MHB in full strength and diluted (50%, 25%, 10%, and 5%) and incubated for 18–24 h at 37 °C (22–24). The considered MIC was the lowest peptide concentration that completely inhibited the growth of each bacterial strain, compared with the growth in the control tube.

Hemolytic activity (HA)

Human erythrocytes were isolated from heparinized blood by centrifugation (1006 × ***g*** for 10 min) after washing three times with saline solution. Erythrocyte solutions were prepared to a concentration of 0.4% (v/v) in isotonic saline solution.

Test-tubes containing 200 μL of erythrocyte solution were incubated at 37 °C for 60 min with 200 μL of peptide solution at concentrations ranging from 50 to 400 μM.

After centrifugation at 1006 × ***g*** for 5 min, the supernatant absorbance was measured at 405 nm. Lysis induced by 1% Triton X-100 was taken as 100%.

Phospholipid–PDA vesicles

Dipalmitoylphosphatidylcholine (DPPC), dipalmitoylphosphatidylglycerol (DPPG), and cholesterol (Chol) were purchased from Sigma (St. Louis, MO, USA). The diacetylenic monomer 10,12-tricosadyinoic acid was provided by Fluka. Tris (hydroxymethylaminomethane) was purchased from Sigma.

Lipid components and the monomeric unit 10,12-tricosadyinoic acid were used at the following mole ratios: DPPG/PDA (4:6), DPPC/PDA

Table 1: Sequences and characterization of the investigated peptides

Analog identification	Region	Sequence	Molecular mass (Da) Calculated	Molecular mass (Da) Experimental[a]	Net charge At pH = 7.4	RP-HPLC Retention time (min)[b]
Pln 149 a	1–22	YSLQMGATAIKQVKKLFKKKGG-NH_2	2424	2423.48	+7	19.7
CT	6–22	GATAIKQVKKLFKKKGG- NH_2	1801.3	1801.25	+6	17.0
C8-CT	6–22	CH_3-$(CH_2)_6$-CO-GATAIKQVKKLFKKKGG- NH_2	1927.52	1927.24	+6	22.1
C12-CT	6–22	CH_3-$(CH_2)_{10}$-CO-GATAIKQVKKLFKKKGG- NH_2	1983.61	1983.21	+6	24.7
CT[W17][c]	6–22	GATAIKQVKKL**W**KKKGG- NH_2	1840.3	1840.11	+6	17.3
C8-CT[W17][c]	6–22	CH_3-$(CH_2)_6$-CO-GATAIKQVKKL**W**KKKGG- NH_2	1966.51	1966.27	+6	21.6

All the peptides are amidated at their C-terminus. Purity >90%.
[a]Determined by Maldi-Tof.
[b]A C_4 column was used, and peptides were eluted in 33 min using a gradient elution of 5–80% of ACN in water containing 0.1% TFA.
[c]Substituted analogs, where Phe17 of Pln149a sequence was replaced by Trp17.

(4:6), DPPC/Chol/PDA (2:2:6), dissolved in chloroform/methanol (1:1) and dried together by purging with N_2 to give a thin film of lipids on the glass surface. Deionized water was added to yield a total lipid concentration of 1 mM. Samples were sonicated at approximately 70 °C followed by slow cooling at 4 °C, overnight. After polymerization by irradiation at 254 nm for 20–30 seconds, vesicles exhibited an intense blue color because of the alternating conjugated triple and double bonds of PDA backbone (25). The self-assembly and photopolymerization of diacetylene compounds after irradiation with UV light have been well documented, and schematic representations of this process appear in different reports (3,7,14,26,27).

Colorimetric measurements

Samples were prepared by adding aqueous peptide solutions to 0.2 mL of vesicle and 2 mM Tris buffer (pH approximately 8). Peptide concentrations in the vesicles ranged from 50 to 350 μM. Finally, the solutions were diluted to 1 mL. UV–Vis spectroscopy measurements were carried out at room temperature on a METROLAB M 1700 spectrophotometer, using a cell of 0.5-cm optical path length.

A quantitative value for the extent of blue-to-red color transitions within the vesicle solutions was given by the colorimetric response (%CR), which was defined as follows (28):

$$\%CR = (PB_0 - PB_I) \times 100/PB_0$$

where

$$PB = Ablue/(Ablue + Ared)$$

A is the absorbance either at the 'blue' component in the UV–Vis spectrum (640 nm) or at the 'red' component (500 nm). PB_0 is the blue/red ratio of the control sample (without peptides), and PB_I is the value obtained for the vesicle solution after colorimetric transition occurs. The reported %CR values were averages of three independent measurements.

The visible spectra of two analogs (Pln149a and C8-CT[W17]) in both phospholipid–PDA systems were included as supplementary data file to show the differences in the colorimetric responses.

Circular dichroism (CD) analysis

Far-UV CD measurements were taken on a Jasco J-810 CD spectrometer (Tokyo, Japan) in a 0.1-cm path quartz curvet (Hellma, Müllheim, Germany) and recorded after accumulation of five runs. CD analyses were recorded in the presence of DPPG and DPPC vesicles. For the preparation of small unilamellar vesicles (SUV), the lipid dispersion in MiliQ water was sonicated until the solution became transparent. The final lipid concentration was 3 mM, and the peptide concentration was 0.2 mg/mL in all samples. Spectra were corrected for background scattering because of the vesicles by subtracting the spectrum of a single vesicle solution to that of the peptides in the presence of vesicles (29,30).

Additional spectra were obtained in water and in the presence of TFE [20 and 40% TFE (v/v)]; final peptide concentration was 0.2 mg/mL in all cases. Deconvolution of CD spectra was performed by CDPro software package (Colorado State University, CO, USA) and CONTINLL method (IBasis 5, 7 and 8) (31–33).

Results and Discussion

The synthesized sequences are shown in Table 1. All CT analogs have a net positive charge of +6. The retention times (rt) of the different peptides determined by reverse HPLC and the experimental molecular mass determined by MALDI-TOF mass spectrometry are also shown in this Table. *N*-terminal acylation increases the rt of the peptides, thus increasing their mean hydrophobicity.

Antimicrobial activity of acylated and substituted CT analogs

In a previous work (18), the antimicrobial activity of Pln149a against two strains of gram (+) bacteria was investigated using full-strength MHB, and unexpected high MIC values were found. In this work, a preliminary study about the antimicrobial activity of Pln149a and its analogs in full-strength and diluted (50%, 25%, 10%, and 5%) MHB was carried out. The results clearly demonstrated that using diluted MHB (10% and 25%) instead of the full-strength medium increased the sensitivity of the antibacterial test. The mid-logarithmic phase of bacterial growth (1×10^4–1×10^5 CFU/mL) was reached in these conditions, and best MIC results were obtained with 10% of MHB. Consequently, MBH diluted at 10% was used in this work for MIC determination.

The effect of MHB strength on the antimicrobial activity of some peptides has been described, and the reduction in the activity when using full-strength medium has been attributed to several factors, like the salt content of the media used to quickly propagate bacterial cultures that blocks the positive charges needed for membrane interaction (34), the aggregation of amphipathic alpha-helical peptides, and/or the interaction of the peptides with other components of this complex media (35). In this way, a good activity of pyrrhocoricin–drosocin dimer chimeras against *S. aureus* was found in one-quarter strength MHB but not in full-strength MHB (36,37).

Also, the effect of different culture media on the antimicrobial activity of short peptides derived of Class IIa bacteriocins against *Listeria* strains has also been reported. The highest antimicrobial activity was detected using chemically defined culture media instead of complex ones. Some components of complex media (like brain heart infusion and MHB) might interfere with detection of the antimicrobial activity (38).

Minimal inhibitory concentration values of the different peptides against *S. aureus* DBFIQ S 21 and *L. monocytogenes* DBFIQ LM3 are shown in Table 2.

The N-terminal conjugation of CT with n-octanoic and n-dodecanoic acids improved the antimicrobial activity against *S. aureus* strain, according to MIC values (C8-CT: 1 μM; C12-CT: 2 μM) (see Table 2).

On the other hand, CT analog showed lower activity against *L. monocytogenes* strain (MIC: 17.8 μM) than to *S. aureus* (MIC: 8.9 μM). A direct correlation between activity and the length of the fatty acid chain conjugated to the peptide was found for *L. monocytogenes* strain, as the best results were obtained when n-dodecanoic acid was used (C12-CT: 4 μM).

Malina & Shai studied the effect of the conjugation of a cationic biologically inactive peptide with fatty acids of different lengths. The conjugation with decanoic acid (C10) and dodecanoic acid (C12) gave rise the most active lipopeptides toward gram (+) and gram (−) bacteria while conjugation with longer fatty acids (myristic and palmitic acid, 14 and 16 carbon atoms) not only decreased the antimicrobial activity but also increased the hemolytic activity (39).

Table 2: Minimal inhibitory concentration (MIC) of peptides against *Staphylococcus aureus* and *Listeria monocytogenes* strains

	MIC (μM)	
	S. aureus	*L. monocytogenes*
Peptide	DBFIQ S21	DBFIQ LM3
Pln 149a	6.6	1.7
CT	8.9	17.8
C8-CT	1.0	16.0
C12-CT	2.0	4.0
CT[W17]	>69.6	69.6
C8-CT[W17]	8.1	8.1

In a recent report, Laverty *et al*. studied the antimicrobial activity of an ultrashort cationic tetrapeptide (OOWW-NH_2), *N*-terminally modified with fatty acids of different length (C6–C16). In this case, tetrapeptides bearing *N*-terminal C12 exhibited optimal antimicrobial activity against bacteria and fungi (40).

The antimicrobial activity of C8-CT and C12-CT against *S. aureus* and *L. monocytogenes* agrees with these reported data in the sense that conjugation with short fatty acid chains appears to be optimal for the interaction of the lipopeptides with the bacterial phospholipid membranes.

However, taking into account that C8-CT and C12-CT differ in their hydrophobicity (see Table 1, rt determined by HPLC), the effect of this physicochemical parameter appears to be more important for the permeabilization of *L. monocytogenes* than for *S. aureus* membranes. Notwithstanding, the most active analog against *L. monocytogenes* strain was Pln149a (MIC: 1.7 μM) (see Table 2).

The action mechanism of Plantaricin A, a bacteriocin that shares significant sequence homology with Plantaricin 149, remains poorly understood, but different studies have suggested that lipid membranes could be a target for its antimicrobial activity against *Listeria* (16).

Then, it appears that the *N*-terminal pentapeptide (YSLQM) of Pln149a favors the interaction with *Listeria* membrane through the hydrophobic amino acid residues Leu3 and Met5. In addition, it is possible that another specific mechanism may be involved in the interaction and permeabilization of *Listeria* membrane.

The substitution of Phe17 by Trp17 significantly reduced the antimicrobial activity of CT against the two tested strains (see Table 2). Nevertheless, CT[W17] conjugation with n-octanoic acid notably increases the antimicrobial activity of this analog against the two tested strains (eightfold more active), showing again that the alkyl chain improves the interaction with the bacterial membranes.

In a study about physicochemical parameters affecting the antimicrobial activity, the hydrophobic moment of the peptide chain was considered as the parameter that has the most significant effect on the antimicrobial activity of lytic peptides (41).

To analyze the substitution effect (Phe17 versus Trp17) on the properties of the sequences, peptide hydrophobicity (H) and hydrophobic moments (Hm) were calculated using the normalized consensus hydrophobicity scale of Eisenberg (42) and the European Molecular Biology Open Software Suite (EMBOSS) (43).

The most amphipathic region of Pln149a is extended from Ile10 to Lys19 (IKQVKKLFKK, Hm: 0.837) and the substitution of Phe by Trp decreases the Hm (0.806) of this region. The mean hydrophobicity of CT and CT[W17] calculated by the same algorithm (H: −0.147 and −0.226, respectively) indicates that CT is slightly more hydrophobic than CT[W17]. In this way, the increased antimicrobial activity of CT against the two gram (+) tested strains may be explained by its higher amphipathicity.

Hemolytic activity

Figure 1A depicts the percent hemolysis of human erythrocytes as a function of peptide concentrations for Pln149a, CT, and its conjugated analogs. Low hemolytic activity was found for Pln149a and almost null for CT in the whole range of concentrations (25–400 μM).

Particularly, at concentrations >100 μM, the differences between the hemolytic activity of C12-CT and the other CT analogs were significantly increased showing that the longer hydrocarbon chain enhances the interaction with the eukaryotic cell membrane. In addition, the different shape of C12-CT curve suggests a different mode of interaction of this analog with the eukaryotic membrane.

The substitution of Phe17 by Trp17 slightly increases the hemolytic activity of CT (not more than 20%) as observed in Figure 1B, but the conjugation of CT[W17] with n-octanoic acid notably increases the cytotoxic activity at concentrations higher than 200 μM.

Circular dichroism (CD) analysis

Circular dichroism results showed that all the peptides adopt a random structure in water as expected for small peptides in aqueous solution, consistent with a pronounced minimum observed around 198 nm and confirmed by deconvolution with CDpro package Program.

In the presence of DPPC vesicles, all the peptides showed a minimum around 200–204 nm, suggesting that they are predominantly unordered (Figure 2A), while in the presence of DPPG vesicles, Pln149a, C8-CT, C12-CT, and C8-CT[W17] showed a predominant α-helical structure with two minima at 208–210 and 217–222 nm and a maximum at 196–198 nm (Figure 2B). This observation also agrees with our previous investigations, indicating that Pln149a adopts α-helical structure in AOT reverse micelles (18), validating the hypothesis that electrostatic interactions between positively charged residues on the peptides and negatively charged groups in the membrane are important for structuring and functionality of these analogs.

Additional CD analyses were carried out in the presence of TFE (20% and 40%). In this case, and for all the peptides, a greater tendency to α-helix structure while increasing TFE concentration was found.

CD studies of Plantaricin A in liposomes have shown that whereas negatively charged membranes induced as much as 45% helicity,

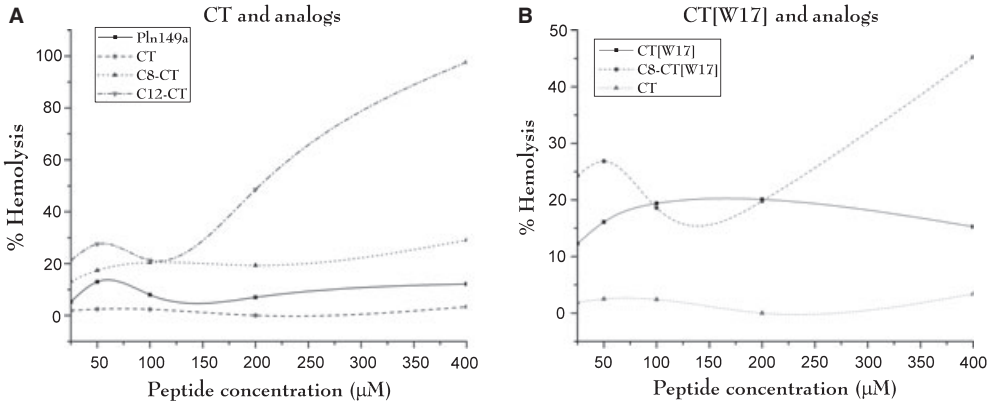

Figure 1: Hemolysis of human erythrocytes as a function of concentration of the different peptide analogs. (A) CT and its fatty acid conjugated analogs. (B) CT and its substituted analogs (Phe17 was replaced by Trp17).

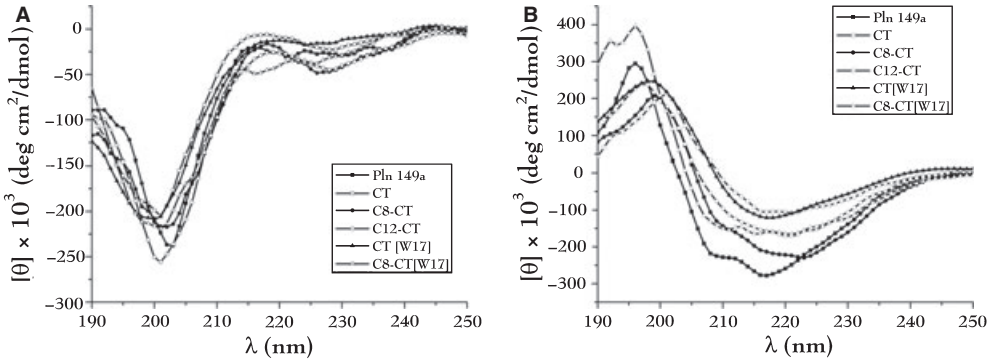

Figure 2: CD spectra of Pln149a, CT acylated and substituted analogs (A) in dipalmitoylphosphatidylcholine vesicles (B) in dipalmitoylphosphatidylglycerol vesicles. Peptide concentration in all measurementes was 0.2 mg/mL.

zwitterionic vesicles induced only around 7% helicity (44). A similar effect of zwitterionic vesicles on Plantaricin E/F and Plantaricin J/K structure was reported (45).

Colorimetric analysis

Figures 3A,B and 4A,B show the colorimetric responses (CR) of lipid/PDA vesicles as a function of peptide concentrations in the biomimetic membranes. The error bars confirm the reproducibility of the colorimetric analysis.

DPPC–Chol–PDA membranes

Figure 3A,B shows the chromatic responses of the peptides interacting with DPPC–Chol–PDA membranes. The shape of the curves of Pln149a, CT, C8-CT, and C12-CT is quite different (see Figure 3A), and only significant differences between the interaction of the lipopeptides compared to CT and Pln149a were observed at high concentrations (225–275 μM). Similarly, a greater interaction of CT[W17] and C8-CT[W17] compared with CT was only observed at concentrations higher than 200 μM (see Figure 3B).

Circular dichroism analyses of the peptides in the presence of DPPC liposomes evidenced they are highly unordered, suggesting a low interaction with zwitterionic membranes, which is also consistent with the low hemolytic activity detected in a wide range of peptide concentrations.

At an early stage, two types of membranes were prepared, one containing DPPC–Chol–PDA and the other without cholesterol. The correlation between hemolytic activity of the peptides and DPPC–PDA interaction was not good when the vesicles were prepared in the absence of cholesterol because high CR values did not correlate with the percentages of hemolysis (data not shown). Instead of this, the addition of cholesterol to DPPC–PDA membranes coincided with a decrease in CR values, suggesting that cholesterol increased the fluidity and stability of the vesicles, leading to a better simulation of human red blood cell membranes.

DPPG–PDA membranes

Figure 4A,B shows the colorimetric responses (CR) of peptides with DPPG–PDA vesicles. Similar shapes of CR curves were found for CT

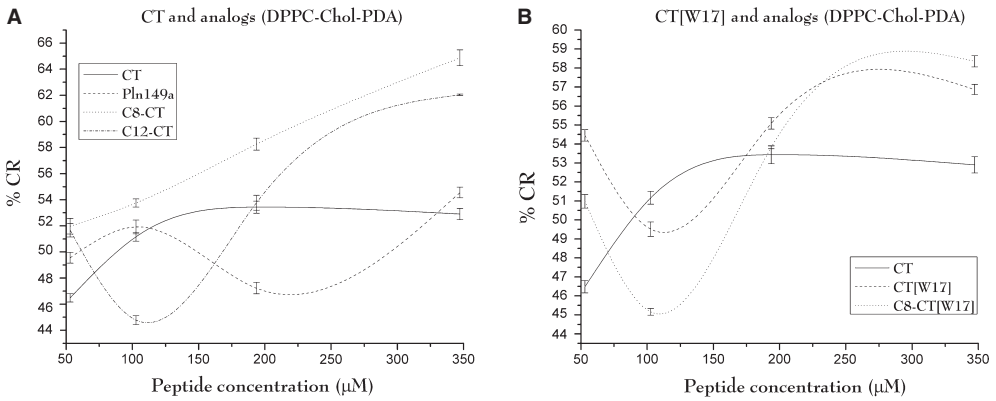

Figure 3: Colorimetric transitions induced in dipalmitoylphosphatidylcholine-Chol-polydiacetylene vesicles for the peptides. (A) Interaction of Pln149a, CT and its conjugated analogs. (B) Interaction of CT and the substituted analogs (Phe17 by Trp17).

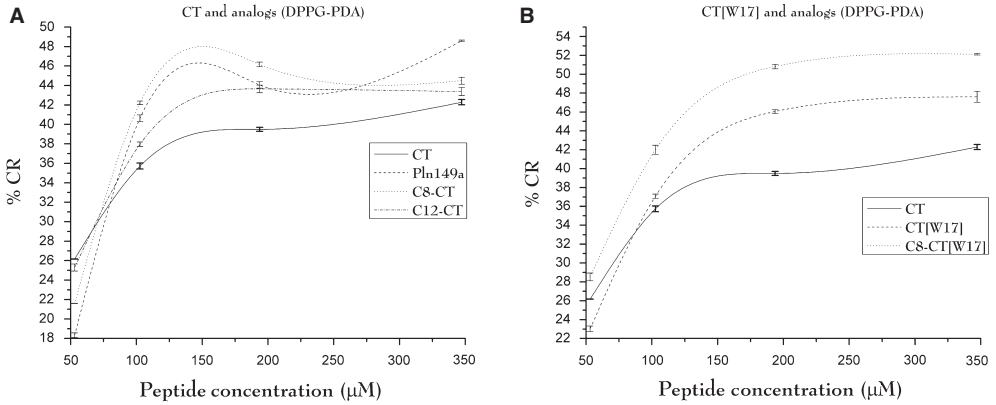

Figure 4: Colorimetric transitions induced in dipalmitoylphosphatidylglycerol-polydiacetylene vesicles. (A) Interaction of Pln149a, CT and its conjugated analogs. (B) Interaction of CT and the substituted analogs (Phe17 by Trp17).

and its conjugated analogs as peptide concentration increased (Figure 4A), also showing that interaction of CT with DPPG–PDA membrane was the lowest in almost the entire range of concentrations tested.

The highest differences between %CR of C8-CT and C12-CT were detected at 150 μM (48% and 43%, respectively), but at higher concentrations (>250 μM), the differences were negligible.

These results correlate with the higher antimicrobial activity of the lipopeptides against the two tested strains, suggesting a better interaction of the lipopeptides with the biomimetic and also with the biological membranes. In the same way, dichroism analyses of lipopeptides have demonstrated that in the presence of anionic vesicles, C8-CT and C12-CT adopt an α-helix structure allowing a high interaction with the bacterial membranes.

The higher interaction of Pln149a with DPPG membranes compared with CT shows that the hydrophobic residues of the N-terminal sequence (YSLQM) improved the interaction with the biomimetic membrane. These results are in agreement with those of antimicrobial activity in the sense that Pln149a was always more active than CT against the two tested strains. Figure 4B shows the interaction of CT, CT[W17], and C8-CT[W17] with DPPG–PDA biomimetic membranes.

The differences in the permeation properties of CT and CT[W17] are not related to distinct structural features as CD analyses in DPPG liposomes evidenced similar contributions of ß-sheet conformation, consistent with the presence of a minimum at 215–216 nm and according to the deconvolution analyses by CDPro software. Nevertheless, these peptides were the least ordered of all investigated peptides. Comparing CT and CT[W17] curves, it was observed that the analog containing Trp gave rise to the steepest increases in %CR in the range of concentrations between 50 and 200 μM. Also, the higher chromatic variations in the %CR values of CT[W17] suggest that this peptide was predominantly located at the lipid–water interface, causing enhanced perturbation in the head-group region of the lipid–polymer assembly. CT, on the other hand, inserted deeper into the hydrophobic core of the lipid bilayer and consequently induced lower %CR. Previous analyses of color transitions induced in phospholipid/PDA systems have verified that surface perturbations are the predominant factors for induction of the PDA color changes (46–49). Such interpretations are also consistent with the hydrogen bonding ability of the Trp indole ring and its preference to locate at the interface membrane (50,51).

Fatty acid acylation of CT[W17] with n-octanoic acid increased the interaction with DPPG–PDA membranes (see Figure 4B), and CD analyses also evidenced that the conjugation promoted a conformation change toward an α-helix structure with minor contributions of ß-sheet, being the structure highly ordered. These results correlate with the biological assays, showing that C8-CT[W17] was the most active substituted analog against the two tested strains.

Colorimetric response values obtained with vesicles of DPPG-PDA varied in a narrow range for the different analogs, according to the concentration of each peptide (35–42% at 100 μM, 200 μM 38–50%), while for DPPC–Chol–PDA vesicles, largest variations were observed, particularly at 200 μM (47–66%), and also higher values of CR were detected with these vesicles.

Different reports have demonstrated that %CR of model peptides varies according to the lipid composition of the vesicles. For example, different %CR were obtained for melittin and indolicin analogs in the presence of DMPC-PDA, DMPE -DMPG-, -PDA, and LPS-DMPC-PDA, among others (8,14,46,47,52). These reports also demonstrated that biomimetic membranes containing DMPC induced higher chromatic responses than those containing DMPG.

Conclusions

Fatty acid acylation increased the interaction with anionic lipid bilayers, and a good correlation was found with the antimicrobial activity, particularly against *S. aureus* strain, suggesting that the hydrocarbon chain improves the interaction with the bacterial membranes. The folding of Pln149a, C8-CT, C12-CT, and C8-CT[W17] into a pronounced helical conformation upon interaction with DPPG vesicles supports from a structural point of view the insertion of these peptides into the bilayer rather than their localization only at the lipid–water interface.

The similar interaction of Pln149a, C8-CT, and C12-CT with DPPG–PDA vesicles could not explain the highest activity of Pln149a against *L. monocytogenes* strain, suggesting that other mechanisms may be also involved in the mode of action against this bacteria.

The random coil structure and low insertion of the peptides in DPPC–PDA vesicles might explain the high selectivity of these peptides toward bacterial membranes.

Acknowledgments

This work was supported by grants from Agencia Nacional de Promoción Científica y Tecnológica (ANPCyT) and Universidad Nacional del Litoral (CAI+D Research Program, 2006 and 2009), República Argentina.

The authors declare that there is no conflict of interest.

References

1. Hancock R.E. (1999) Host defence (cationic) peptides: what is their future clinical potential? Drugs;57:469–473.
2. Charych D., Cheng Q., Reichert A., Kuziemko G., Stroh M., Nagy J.O., Spevak W., Stevens R.C. (1996) A 'litmus test' for molecular recognition using artificial membranes. Chem Biol;3:113–120.
3. Jelinek R., Kolusheva S. (2001) Polymerized lipid vesicles as colorimetric biosensors for biotechnological applications. Biotechnol Adv;19:109–118.
4. Cheng Q., Stevens R.C. (1998) Charge-induced chromatic transition of amino acid-derivatized polydiacetylene liposomes. Langmuir;14:1974–1976.

5. Huo Q., Russell K.C., Leblanc R.M. (1999) Chromatic studies of a polymerizable diacetylene hydrogen bonding self-assembly: a ``self-folding'' process to explain the chromatic changes of polydiacetylenes. Langmuir;15:3972–3980.
6. Huo Q., Russev S., Hasegawa T., Nishijo J., Umemura J., Puccetti G., Russell K.C., Leblanc R.M. (2000) A Langmuir monolayer with a nontraditional molecular architecture. J Am Chem Soc;122:7890–7897.
7. Jonas U., Shah K., Norvez S., Charych D.H. (1999) Reversible color switching and unusual solution polymerization of hydrazide-modified diacetylene lipids. J Am Chem Soc;121:4580–4588.
8. Kolusheva S., Boyer L., Jelinek R. (2000) A colorimetric assay for rapid screening of antimicrobial peptides. Nat Biotechnol;18:225–227.
9. Lio A., Reichert A., Ahn D.J., Nagy J.O., Salmeron M., Charych D.H. (1997) Molecular imaging of thermochromic carbohydrate-modified polydiacetylene thin films. Langmuir;13:6524–6532.
10. Song J., Cheng Q., Kopta S., Stevens R.C. (2001) Modulating artificial membrane morphology: pH-induced chromatic transition and nanostructural transformation of a bolaamphiphilic conjugated polymer from blue helical ribbons to red nanofibers. J Am Chem Soc;123:3205–3213.
11. Deckert A.A., Horne J.C., Valentine B., Kiernan L., Fallon L. (1995) Effects of molecular area on the polymerization and thermochromism of Langmuir-Blodgett films of Cd2 + salts of 5,7-diacetylenes studied using UV-Visible spectroscopy. Langmuir;11:643–649.
12. Mino N., Tamura H., Ogawa K. (1991) Analysis of color transitions and changes on Langmuir-Blodgett films of a polydiacetylene derivative. Langmuir;7:2336–2341.
13. Nallicheri R.A., Rubner M.F. (1991) Investigations of the mechanochromic behavior of poly(urethane-diacetylene) segmented copolymers. Macromolecules;24:517–525.
14. Kolusheva S., Shahal T., Jelinek R. (2000) Peptide-membrane interactions studied by a new phospholipid/polydiacetylene colorimetric vesicle assay. Biochemistry;39:15851–15859.
15. Kolusheva S., Wachtel E., Jelinek R. (2003) Biomimetic lipid/polymer colorimetric membranes: molecular and cooperative properties. J Lipid Res;44:65–71.
16. Zhao H., Sood R., Jutila A., Bose S., Fimland G., Nissen-Meyer J., Kinnunen P.K. (2006) Interaction of the antimicrobial peptide pheromone Plantaricin A with model membranes: implications for a novel mechanism of action. Biochim Biophys Acta;1758:1461–1474.
17. Kato T., Matsuda T., Ogawa E., Ogawa H., Kato H., Doi U., Nakamura R. (1994) Plantaricin-149, a bacteriocin produced by Lactobacillus plantarum NRIC 149. J Ferment Bioeng;77:277–282.
18. Muller D.M., Carrasco M.S., Simonetta A.C., Beltramini L.M., Tonarelli G.G. (2007) A synthetic analog of plantaricin 149 inhibiting food-borne pathogenic bacteria: evidence for alpha-helical conformation involved in bacteria-membrane interaction. J Pept Sci;13:171–178.
19. Lopes J.L., Nobre T.M., Siano A., Humpola V., Bossolan N.R., Zaniquelli M.E., Tonarelli G., Beltramini L.M. (2009) Disruption of Saccharomyces cerevisiae by Plantaricin 149 and investigation of its mechanism of action with biomembrane model systems. Biochim Biophys Acta;1788:2252–2258.
20. Ghosh B.K., Carroll K.K. (1968) Isolation, composition, and structure of membrane of *Listeria monocytogenes*. J Bacteriol;95:688–699.
21. White D.C., Frerman F.E. (1968) Fatty acid composition of the complex lipids of *Staphylococcus aureus* during the formation of the membrane-bound electron transport system. J Bacteriol;95:2198–2209.
22. Amsterdam D. (1996) Susceptibility testing of antimicrobials in liquid media. In: Lorian V., editor. Susceptibility testing of antimicrobials in liquid media. Baltimore, MD: Williams & Wilkins; p. 52–111.
23. Steinberg D.A., Hurst M.A., Fujii C.A., Kung A.H., Ho J.F., Cheng F.C., Loury D.J., Fiddes J.C. (1997) Protegrin-1: a broad-spectrum, rapidly microbicidal peptide with in vivo activity. Antimicrob Agents Chemother;41:1738–1742.
24. Wu M., Hancock R.E. (1999) Interaction of the cyclic antimicrobial cationic peptide bactenecin with the outer and cytoplasmic membrane. J Biol Chem;274:29–35.
25. Okada S.Y., Jelinek R., Charych D. (1999) Induced color change of conjugated polymeric vesicles by interfacial catalysis of phospholipase A2. Angew Chem Int Edit;38:655–659.
26. Volinsky R., Kolusheva S., Berman A., Jelinek R. (2006) Investigations of antimicrobial peptides in planar film systems. Biochim Biophys Acta;1758:1393–1407.
27. Vinod T.P., Chang J.H., Kim J.W., Rhee S.W. (2008) Self-assembly and photopolymerization of diacetylene molecules on surface of magnetite nanoparticles. Bull Korean Chem Soc;29:799–804.
28. Jelinek R., Okada S., Norvez S., Charych D. (1998) Interfacial catalysis by phospholipases at conjugated lipid vesicles: colorimetric detection and NMR spectroscopy. Chem Biol;5:619–629.
29. Ladokhin A.S., Fernández-Vidal M., White S.H. (2010) CD spectroscopy of peptides and proteins bound to large unilamellar vesicles. J Membr Biol;236:247–253.
30. Huang C. (1969) Studies on phosphatidylcholine vesicles. Formation and physical characteristics. Biochemistry;8:344–352.
31. Chen Y.H., Yang J.T. (1971) A new approach to the calculation of secondary structures of globular proteins by optical rotatory dispersion and circular dichroism. Biochem Biophys Res Commun;44:1285–1291.
32. Sreerama N., Venyaminov S.Y., Woody R.W. (2000) Estimation of protein secondary structure from circular dichroism spectra: inclusion of denatured proteins with native proteins in the analysis. Anal Biochem;287:243–251.
33. Sreerama N., Woody R.W. (2000) Estimation of protein secondary structure from circular dichroism spectra: comparison of CONTIN, SELCON, and CDSSTR methods with an expanded reference set. Anal Biochem;287:252–260.
34. Bulet P., Urge L., Ohresser S., Hetru C., Otvos L. Jr (1996) Enlarged scale chemical synthesis and range of activity of drosocin, an O-glycosylated antibacterial peptide of Drosophila. Eur J Biochem;238:64–69.
35. Zelezetsky I., Pacor S., Pag U., Papo N., Shai Y., Sahl H.G., Tossi A. (2005) Controlled alteration of the shape and conformational stability of alpha-helical cell-lytic peptides: effect on mode of action and cell specificity. Biochem J;390:177–188.
36. Otvos L., Snyder C., Condie B., Bulet P., Wade J. (2005) Chimeric antimicrobial peptides exhibit multiple modes of action. Int J Pept Res Ther;11:29–42.

37. Otvos L., Cudic M. (2007) Broth microdilution antibacterial assay of peptides. In: Fields G., editor. Methods in molecular Biology, vol. 386: Peptide characterization and application protocols. Totowa, NJ: Humana Press Inc.; p. 309–320.
38. Salvucci E., Saavedra L., Sesma F. (2007) Short peptides derived from the NH2-terminus of subclass IIa bacteriocin enterocin CRL35 show antimicrobial activity. J Antimicrob Chemother;59:1102–1108.
39. Malina A., Shai Y. (2005) Conjugation of fatty acids with different lengths modulates the antibacterial and antifungal activity of a cationic biologically inactive peptide. Biochem J;390:695–702.
40. Laverty G., McLaughlin M., Shaw C., Gorman S.P., Gilmore B.F. (2010) Antimicrobial activity of short, synthetic cationic lipopeptides. Chem Biol Drug Des;75:563–569.
41. Pathak N., Salas-Auvert R., Ruche G., Janna M.H., McCarthy D., Harrison R.G. (1995) Comparison of the effects of hydrophobicity, amphiphilicity, and alpha-helicity on the activities of antimicrobial peptides. Proteins;22:182–186.
42. Eisenberg D., Weiss R.M., Terwilliger T.C. (1984) The hydrophobic moment detects periodicity in protein hydrophobicity. Proc Natl Acad Sci USA;81:140–144.
43. Rice P., Longden I., Bleasby A. (2000) EMBOSS: the European Molecular Biology Open Software Suite. Trends Genet;16:276–277.
44. Hauge H.H., Mantzilas D., Moll G.N., Konings W.N., Driessen A.J., Eijsink V.G., Nissen-Meyer J. (1998) Plantaricin A is an amphiphilic alpha-helical bacteriocin-like pheromone which exerts antimicrobial and pheromone activities through different mechanisms. Biochemistry;37:16026–16032.
45. Hauge H.H., Mantzilas D., Eijsink V.G., Nissen-Meyer J. (1999) Membrane-mimicking entities induce structuring of the two-peptide bacteriocins plantaricin E/F and plantaricin J/K. J Bacteriol;181:740–747.
46. Halevy R., Rozek A., Kolusheva S., Hancock R.E., Jelinek R. (2003) Membrane binding and permeation by indolicidin analogs studied by a biomimetic lipid/polydiacetylene vesicle assay. Peptides;24:1753–1761.
47. Sheynis T., Sykora J., Benda A., Kolusheva S., Hof M., Jelinek R. (2003) Bilayer localization of membrane-active peptides studied in biomimetic vesicles by visible and fluorescence spectroscopies. Eur J Biochem;270:4478–4487.
48. Volinsky R., Kolusheva S., Berman A., Jelinek R. (2004) Microscopic visualization of alamethicin incorporation into model membrane monolayers. Langmuir;20:11084–11091.
49. Dorosz J., Gofman Y., Kolusheva S., Otzen D., Ben-Tal N., Nielsen N.C., Jelinek R. (2010) Membrane interactions of novicidin, a novel antimicrobial peptide: phosphatidylglycerol promotes bilayer insertion. J Phys Chem B;114:11053–11060.
50. Sun H., Greathouse D.V., Andersen O.S., Koeppe R.E. II (2008) The preference of tryptophan for membrane interfaces: insights from N-methylation of tryptophans in gramicidin channels. J Biol Chem;283:22233–22243.
51. Yau W.M., Wimley W.C., Gawrisch K., White S.H. (1998) The preference of tryptophan for membrane interfaces. Biochemistry;37:14713–14718.
52. Katz M., Tsubery H., Kolusheva S., Shames A., Fridkin M., Jelinek R. (2003) Lipid binding and membrane penetration of polymyxin B derivatives studied in a biomimetic vesicle system. Biochem J;375:405–413.